Band alignment of III-N, ZnO and II-IV-N$_2$ semiconductors from the electron affinity rule

Sai Lyu‡, and Walter R. L. Lambrecht

Department of Physics, Case Western Reserve University, 10900 Euclid Avenue, Cleveland, Ohio 44106-7079, USA

E-mail: `sai.lyu@case.edu and walter.lambrecht@case.edu`

Abstract.   The natural band alignment between various II-IV-N$_2$ and III-N and ZnO semiconductors are determined by means of first-principles surface calculations of their electron affinities. While these ignore specific interface dipole formation and strain effects, they provide a first guidance to the construction of heterojunction devices involving this family of materials.

‡ Current address: Chaire de Simulation à l' Échelle Atomique (CSEA), École Polytechnique Fédérale de Lausanne, 1015 Lausanne, Switzerland

1. Introduction

The simplest and oldest model for heterojunction band-offsets between semiconductors is the electron affinity rule, attributed to Anderson[1] and closely related to the Schottky-Mott rule for metal/semiconductor interfaces. It states that the conduction band offset is given by the difference in the electron affinities, $\Delta E_c = E_{c2} - E_{c1} = \chi_2 - \chi_1$, where the electron affinity $\chi = E_{vac} - E_c$ is the energy difference from the vacuum level just outside the material to the conduction band minimum. In other words, it assumes the vacuum level can be aligned and when bringing the two materials in contact, no significant charge transfer from one to the other (interface dipole formation) occurs. Obviously, this is usually not true and several improved models have been proposed for abrupt and heterojunctions with close lattice match taking into the account the dipole formation at the interface[2, 3, 4, 5] .The crucial point is that the band-offset is a discontinuity which occurs at atomistic length-scale. It is independent of the doping in each of the materials and the space charge depletion zone formation in each will at a macroscopic scale align the Fermi levels and determine the built-in potentials at the junction, which determines their rectifying behavior.

In spite of the obvious limitations of the electron affinity rule, it has remained a useful and widely used model for obtaining a first rough idea of the band alignment between two dissimilar materials and provides guidance for designing device structures, such as electron and hole extraction layers in solar cells. One reason may be that in contrast to precisely defined specific surface orientation abrupt and coherent semiconductor interfaces, one often encounters less well characterized, less well bonded interfaces. In fact, at an interface between two polycrystalline films, even different relative interface orientations may exist and would have to be averaged over. The notion of a band position of each material relative to a common vacuum level ignoring the specific interface dipoles then starts to make more physical sense.

Even for a well defined interface orientation, when the lattice mismatch is large and the films exceed a critical thickness, typically misfit dislocations form to relieve the interface strain. These are only rarely taken into account explicitly in the band offset evaluation[6]. Instead, one avoids the interface strain by introducing the concept of a "natural band offset" as the offset that would exist between two unstrained materials assuming the electron-affinity rule[7, 8]. This then forms a comparison point for specific interfaces, and allows one to separate the role of interface dipoles and strain in each material, which can be determined using deformation potentials and the specific strain state the material is in, from the intrinsic or natural offset.

On the other hand, it is well known that density functional theory (DFT) Kohn-Sham energy bands do not well represent one-particle excitations and for example fail to give accurate band gaps. A better approach in principle is to use many-body perturbation theory such as Hedin's GW approximation for the self-energy, where G is the one-electron Green's function and W the screened Coulomb interaction. An important question is then how well different levels of theory (DFT with semi-local or

hybrid functionals, *GW* theory) determine the positions of energy levels with respect to the vacuum level and from them the natural band-offsets [9, 10, 11] .

Here we present natural band-offsets for a number of members of the family of II-IV-N$_2$ semiconductors, which are closely related to the III-N semiconductors. This family of materials has thus far received limited attention but has been found to be a natural and possibly useful extension of the well-studied group-III nitrides [12, 13]. They have similar tetrahedral bonding and a wurtzite derived crystal structure in which each N is coordinated by an octet-rule preserving arrangement of two group-II and two group-IV atoms instead of four group III atoms. Some previous calculations of band-offsets[14] predicted a large band offset between GaN and ZnGeN$_2$ in spite of the two materials having very close band gaps. This leads to a staggered (type-II) band offset which was subsequently found to be useful to improve the design of light-emitting diode (LED) device structures by shaping the wave function of the holes and electrons and thereby creating a larger overlap between them, which was predicted to increase the efficiency by a significant factor (6–7) [15, 16]. Other advantages of the combination of II-IV-N$_2$ with III-N materials were demonstrated computationally for intersubband transitions in quantum cascade laser structures [17]. To design future device structures involving the by now significantly expanded family of II-IV-N$_2$ materials, it is important to have at least a first guidance to their band alignment. The natural band offsets, in spite of their limitation to predict the interface specific dipoles provide a good framework for this purpose.

2. Computational method

Our calculations are based on Density Functional Theory(DFT)[18, 19] in the Local Density Approximation (LDA) and the Quasiparticle Self-consistent (QS) *GW* method[20, 21]. The lattice parameters are determined using total energy minimization using the Broyden-Flectcher-Goldfard-Shanno (BFGS) minimization method [22] in the ABINIT package. The BFGS method can simultaneously determine cell shape and atomic positions by using the stress tensor. We used the Projector Augmented Wave (PAW) method and pseudopotentials to account for the interaction between nuclei and electron. For InN and GaN, PAW[23] atomic data extracted from ultra-soft pseudopotential (USPP) [24] are used and the plane-wave (PW) basis set with energy cutoff of 20 Ha, and a $8 \times 8 \times 4$ **k**-point mesh is used to sample the Brillouin zone. For II-IV-N$_2$ compounds, we adopt Hartwigsen-Goedecker-Hutter HGH pseudopotentials[25], a 80-Ha PW kinetic energy cutoff, and a $4 \times 4 \times 4$ **k**-point mesh. The forces are relaxed to a maximum of 4×10^{-4} Hartree/Bohr.

We use the full-potential linearized muffin-tin orbital method [26, 27] implemented in the QUESTAAL package (https://questaal.org) to calculate the electronic band structure in the QS*GW* approximation. In the *GW* approximation, the self-energy $\Sigma = iGW$ is schematically given by product of G and W. G and W stand for Green's function and screened Coulomb interaction, respectively. In its quasiparticle

self-consistent (QS) version, the energy dependent self-energy $\Sigma(\omega)$ is used to extract a new exchange-correlation potential $\tilde{\Sigma}_{ij} = \frac{1}{2}\text{Re}[\Sigma_{ij}(\epsilon_i) + \Sigma_{ij}(\epsilon_j)]$ expressed in the basis of eigenstates of the independent particle Hamiltonian H_0 from which the G_0 and W_0 and hence Σ are derived, and which is then made self-consistent. This determines the optimum H_0 from which to obtain the best G_0W_0 self-energy and makes the method independent of starting point. The Kohn-Sham eigenvalues of H_0 at self-consistency coincide with the quasiparticle excitation energies of the GW method. The QSGW method tends to systematically overestimates the band gaps for semiconductors because of the underestimate of dielectric screening. This can be further improved by mixing 80% of the Σ and 20% of the LDA exchange-correlational functional v_{xc}, which gives more accurate band gap values. The detailed justification of this renormalization can be found in [28].

Ionization potential (IP) and electron affinity (EA) are defined to be the negatives of the VBM and CBM relative to vacuum level, respectively. The IP and EA are evaluated by combining periodic bulk and slab calculations. Essentially, we use a DFT calculation to determine the electrostatic potential profile at the surface and the GW calculations of the bulk to determine the band edge positions relative to the electrostatic potential. More specifically, the average over the atoms in the cell of the potential at the muffin-tin radii serves as potential marker with respect to which we can determine the band edge positions in a bulk calculation either in the DFT or GW approximation. The same potential average is then evaluated in the center of a slab with respect to the vacuum level outside the slab and called R_v. By adding to it the VBM$_{DFT}$ calculated in bulk we obtain the valence band positions relative to the vacuum level.

The muffin-tin radius potential average[14] is taken in proportion to the sphere areas:

$$\bar{V} = \frac{\sum_i V_i r_i^2}{\sum_i r_i^2} \tag{1}$$

where V_i denotes the muffin-tin potential at radius r_i of the i-th atom and the sum runs over all the atoms within one layer. This methodology is similar to that used in Refs. [29, 10]. In the slab calculation, both the slab thickness and the size of the vacuum region should be large enough to ensure that the electron density and therefore electrostatic potential in the central region of the slab are the same as those in the periodic bulk material. The slab thickness chosen here is 12 layers separated by the equivalent of 10 layers of vacuum. To extract the vacuum level, *i.e.* the electrostatic potential in the vacuum region, we put empty muffin-tin spheres in the vacuum region whose boundary potentials are regarded as vacuum levels. The GW shift

$$\Delta_{VBM} = \text{VBM}_{GW} - \text{VBM}_{DFT} \tag{2}$$

is used to incorporate the GW-level energy bands along with the DFT determined electrostatic potentials relative to vacuum. All calculations are done starting from LDA exchange-correlation functionals. In short,

$$\text{VBM}_{GW,v} = R_v + \text{VBM}_{DFT} + \Delta_{VBM} \tag{3}$$

Table 1. Band gaps in 0.8Σ QSGW approximation, VBM$_{DFT}$ position of DFT-VBM relative to internal electrostatic potential in bulk, R_v internal electrostatic potential relative to vacuum, Δ_{VBM}, VBM shift due to GW, VBM$_{GW,v}$ and CBM$_{GW,v}$ levels relative to vacuum level, for ZnO and III-N and II-IV-N$_2$ compounds.

	0.8Σ gap (direct)	VBM$_{DFT}$	R$_v$	Δ_{VBM}	VBM$_{GW,v} = -$IP	CBM$_{GW,v} = -\chi$
ZnO	3.50	0.05	-7.63	-1.29	-8.87	-5.37
ZnO(m-plane)	3.50	0.05	-7.63	-1.29	-8.87	-5.37
GaN	3.54	2.75	-11.08	-0.21	-8.54	-5.00
GaN(m-plane)	3.54	2.75	-11.13	-0.21	-8.59	-5.05
InN	0.77	2.11	-9.53	0.07	-7.35	-6.58
InN(m-plane)	0.77	2.11	-9.49	0.07	-7.31	-6.54
MgSiN$_2$	6.30	3.97	-13.29	-0.55	-9.87	-3.57
MgGeN$_2$	4.71	3.08	-11.55	-0.39	-8.86	-4.15
MgSnN$_2$	2.62	2.33	-10.45	-0.18	-8.30	-5.68
ZnSiN$_2$	5.83	4.69	-13.55	-0.54	-9.40	-3.57
ZnGeN$_2$	3.62	3.69	-11.45	-0.29	-8.05	-4.43
ZnSnN$_2$	1.86	2.69	-9.92	-0.21	-7.44	-5.58
CdSiN$_2$	3.82	4.16	-12.30	-0.27	-8.41	-4.59
CdGeN$_2$	2.71	3.00	-10.42	-0.19	-7.61	-4.90
CdSnN$_2$[a]	0.84	2.19	-9.13	0.21	-6.73	-5.89

[a] The band gaps for Cd-IV-N$_2$ compounds are taken from Reference [30].
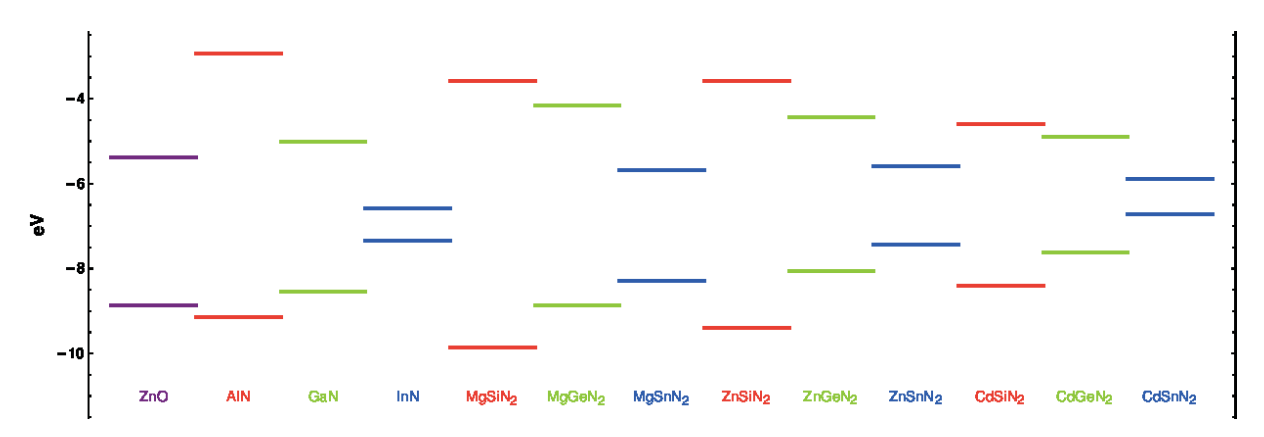

Figure 1. VBM and CBM levels with respect to vacuum level for ZnO and III-N and II-IV-N$_2$ compounds.

By adding the gap we obtain the electron affinities.

3. Results and Discussions

The natural band offset determined via the electron affinity rule is still surface orientation specific. Here we pick the **a**-plane because it is a charge neutral or non-polar

Table 2. Valence band offsets.

	ZnO	GaN	InN	MgSiN$_2$	MgGeN$_2$	MgSnN$_2$	ZnSiN$_2$	ZnGeN$_2$	ZnSnN$_2$	CdSiN$_2$	CdGeN$_2$	CdSnN$_2$
ZnO		0.33	1.52	-1.00	0.01	0.57	-0.53	0.82	1.43	0.46	1.26	2.14
GaN			1.19	-1.33	-0.32	0.24	-0.86	0.49	1.10	0.13	0.93	1.81
InN				-2.52	-1.51	-0.95	-2.05	-0.70	-0.09	-1.06	-0.26	0.62
MgSiN$_2$					1.01	1.57	0.47	1.82	2.43	1.46	2.26	3.14
MgGeN$_2$						0.56	-0.54	0.81	1.42	0.45	1.25	2.13
MgSnN$_2$							-1.10	0.25	0.86	-0.11	0.69	1.57
ZnSiN$_2$								1.35	1.96	0.99	1.79	2.67
ZnGeN$_2$									0.61	-0.36	0.44	1.32
ZnSnN$_2$										-0.97	-0.17	0.71
CdSiN$_2$											0.80	1.68
CdGeN$_2$												0.88

Table 3. Conduction band offsets.

	ZnO	GaN	InN	MgSiN$_2$	MgGeN$_2$	MgSnN$_2$	ZnSiN$_2$	ZnGeN$_2$	ZnSnN$_2$	CdSiN$_2$	CdGeN$_2$	CdSnN$_2$
ZnO		0.37	-1.21	1.80	1.22	-0.31	1.80	0.94	-0.21	0.78	0.47	-0.52
GaN			-1.58	1.43	0.85	-0.68	1.43	0.57	-0.58	0.41	0.10	-0.89
InN				3.01	2.43	0.90	3.01	2.15	1.00	1.99	1.68	0.69
MgSiN$_2$					-0.58	-2.11	0.00	-0.86	-2.01	-1.02	-1.33	-2.32
MgGeN$_2$						-1.53	0.58	-0.28	-1.43	-0.44	-0.75	-1.74
MgSnN$_2$							2.11	1.25	0.10	1.09	0.78	-0.21
ZnSiN$_2$								-0.86	-2.01	-1.02	-1.33	-2.32
ZnGeN$_2$									-1.15	-0.16	-0.47	-1.46
ZnSnN$_2$										0.99	0.68	-0.31
CdSiN$_2$											-0.31	-1.30
CdGeN$_2$												-0.99

plane. The results for the QSGW gap in the 0.8Σ approximation, the valence band maximum and conduction band minima locations relative to vacuum and the above defined R_v and VBM$_{DFT}$ and Δ_{VBM} are given in Table 1. From this table the natural valence band offset can be obtained between any pair of compounds. For convenience, these are summarized in Tables 2,3 and shown in Figure 1. Besides the Zn-IV-N$_2$, Mg-IV-N$_2$ and Cd-IV-N$_2$ families we include the III-N materials GaN, and InN and ZnO because these are likely to be used as substrates for growth of the II-IV-N$_2$. For the III-N and ZnO wurtzite materials, we also give the m-plane values to allow one to test the predictions of the electron affinity rule for that plane for the III-N and ZnO. In fact, we can see that for both of these non-polar planes, the ionization potentials and electron affinities are very close to each other, the deviations being less than 0.05 eV. The band gap values of the Mg-IV-N$_2$ compounds were first reported in Reference [31] but recently corrected for the Ge and Sn case to include the effect of the Ge and Sn semicore levels [32]. In Figure 1 we also included AlN by relating its VBM and CBM levels to GaN [33, 34].

Comparing the present natural band offsets for the [100] or **a**-plane with those of Punya *et al* [14, 35], we see that for GaN/ZnGeN$_2$ we here obtain 0.49 eV while that work gave 1.30 eV. This shows that the charge transfer interface dipole effects are not negligible. Nonetheless the electron affinity rule already correctly predicts the VBM of ZnGeN$_2$ to be above that of GaN and this can be understood from the fact that in ZnGeN$_2$, the Zn-$3d$ states push the VBM up more than the Ga-$3d$ states do in GaN.

Another interesting example is ZnO/GaN. This case was indirectly also studied by Punya *et al* [14, 35] by using the transitivity rule and using the calculated ZnO/ZnGeN$_2$ and GaN/ZnGeN$_2$ offsets removing the specific strain effects from each of these to obtain "natural" band-offsets. The $\Delta E_v(\mathrm{GaN/ZnO}) = 0.6$ eV is obtained in this way while here we find only 0.33 eV. This indicates that even after strain effects were explicitly removed, the results of such indirectly obtained offsets (via the transitivity rule) still depend on the interface dipoles obtained for each explicitly calculated interface. The previous work on that offset was discussed in some detail in Reference [14]. Photoemission measurements by Liu *et al* [36] gave 0.7 eV as band offset, showing that the actual interface calculation is closer to experiment. An even larger value 1.31 eV was obtained by Wang *et al* [37] using HSE and using explicit calculations of ZnO/ZnSnN$_2$ and GaN/ZnSnN$_2$. However, these rely on specific treatment of the strain assuming in-plane lattice match to the substrate and the volume of the film would not change. The latter assumption is incorrect, the films should relax so as to minimize total energy not to maintain volume/formula unit. Obviously, different strain relaxations would then occur at a ZnO/GaN interface and thus, the use of the transitivity rule is not well justified if one does not remove these specific strain effects by considering the "natural band-offset". They nonetheless claimed good agreement with another experimental value of 1.37 eV, which was also obtained indirectly via the transitivity rule [38]. We thus strongly caution against the indiscriminate use of the transitivity rule for band offsets. This makes sense only if the three materials are closely lattice matched or one removes in some way the strain and interface specific dipole effects for each pair before predicting the third band offset. It is clearly obeyed for natural band-offsets but not for specifically strained pairs of band offsets.

However, we should keep in mind that here our goal is not so much to provide specific interface band offsets which depend obviously on many detailed factors, such as abruptness of the interface, strain state of the film, interface orientation, degree of charge transfer, etc. but rather the "natural band-offset" obtained from the electron affinity rule or the ionization potentials. It is thus perhaps more interesting to compare with the results from Reference [9]. From their supplemental material, the IP for GaN, ZnO are 6.61 eV and 7.11 eV in HSE and after including their recommended test-charge test-charge GW correction ΔGW^{TC-TC}, they become 7.296, 8.236 eV. Our value for the ZnO IP is 8.87 eV and for GaN it is 8.54 eV, both larger than their values. They quote experimental values of 6.60–6.80 eV for the ionization potential of GaN and 7.82 for ZnO. Both are smaller than the calculated values. The resulting ZnO/GaN band offsets in their approach vary from 0.50 eV to 0.94 eV depending on whether one takes the

HSE or GW corrected values and compare with a value of 1.02–1.20 eV deduced from the experimental IP values. So, there are still numerous discrepancies but nonetheless both our work and theirs agrees that the *GW* correction to the band offset is larger for ZnO than for GaN. In fact, ZnO, is a notoriously difficult case to converge even the band gaps,[39] let alone the more difficult IP with respect to the number of empty bands included when using plane wave basis sets in *GW*. This problem is avoided in our *GW* implementation because of the use of a mixed product basis set basis set for expanding two-point quantities like polarization and screened Coulomb interaction W [21].

For GaN/ZnSnN$_2$, we here obtain 1.10 eV and the previous work gave 1.64 eV. Our previous work considered specific interfaces and the effects of strain and should thus be considered more accurate for the specific case of a thin film ZnSnN$_2$ epitaxially grown on GaN and thin enough to avoid misfit dislocation formation. In contrast, Wang *et al* [37] obtained a value of only 0.39 eV for another assumption on the strains. It shows that for these specific interfaces, the interface dipole formation and strain effects are non-negligible. Nonetheless, the simple electron affinity rule still shows a fairly large positive band offset in both cases. For ZnSnN$_2$ relative to GaN, the band-offset is in good agreement with the value of Arca *et al* [40] which is essentially determined in the same way using the electron affinity rule but using experimental data. They estimate the valence band offset to be between 1.0 and 1.3 eV depending on which value is used for the ionization potential of GaN. The absolute position of the VBM of ZnSnN$_2$ relative to vacuum in our work is -7.44 eV while in Arca *et al* [40] it was measured to be -5.6 eV. The experimental values for the electron affinity of GaN show significant spread but are also about 1 eV larger than our calculated value of -5.0 eV. Thus while in both cases, the absolute values of the ionization potentials differ from experiment by ~ 1 eV, the band offset comes out in good agreement with experiment.

Generally speaking, Grüneis *et al* [9] found that the ionization potentials of semiconductors are overestimated by DFT in the semilocal generalized gradient approximation (GGA) but underestimated by the GW$_0$ approximation starting from that GGA approximation. They argued that vertex corrections are required to correct this. Our present QS*GW* calculations confirm that both for GaN and ZnO the ionization potential is underestimated. On the other hand the DFT values for ZnO and GaN would be 7.58 eV and 8.33 which both overestimate the experimental values. Thus our results are in agreement with previously observed trends. In spite of the problem with predicting absolute values of the ionization potentials intrinsic to the DFT and even *GW* results, these errors are likely to be largely systematic and thus the values can still be used to determine band offsets keeping the overall limitations of the approach in mind that specific interface dipoles are not included in the method.

Examining the trends in Figure 1 we see type-I offsets within each family of Mg-IV-N$_2$, Zn-IV-N$_2$ and Cd-IV-N$_2$ with the VBM level each time rising from Si to Ge to Sn as group-IV element. The same trend is seen from Al to Ga to In. Relative to GaN, MgGeN$_2$ shows a type-I offset while ZnGeN$_2$ and CdGeN$_2$ show a staggered type-II offset.

4. Conclusion

In this paper, we have presented ionization potentials and electron affinities which can be used to determine natural band offsets for the families of the III-N and II-IV-N$_2$ semiconductors and ZnO. Good agreement with previous work is found keeping the limitations of the approach in mind. We hope that the present extended set of band-offsets in the whole family will be useful for initial design of heterostructures involving these materials. From the specific examples discussed in detail, however, it is clear that interface dipole formation specific to each pair of materials are not negligible and thus, actual interface calculations taking into account the specific strain state of both materials will be required to make more accurate predictions of the band offset for any pair of materials one is interested in further pursuing.

Acknowledgments

[1] Anderson R 1962 *Solid-State Electronics* **5** 341 – 351 ISSN 0038-1101 URL http://www.sciencedirect.com/science/article/pii/0038110162901156
[2] Tersoff J 1984 *Phys. Rev. B* **30**(8) 4874–4877 URL https://link.aps.org/doi/10.1103/PhysRevB.30.4874
[3] Van de Walle C G and Martin R M 1987 *Phys. Rev. B* **35**(15) 8154–8165 URL https://link.aps.org/doi/10.1103/PhysRevB.35.8154
[4] Lambrecht W R L and Segall B 1988 *Phys. Rev. Lett.* **61**(15) 1764–1767 URL https://link.aps.org/doi/10.1103/PhysRevLett.61.1764
[5] Lambrecht W R L, Segall B and Andersen O K 1990 *Phys. Rev. B* **41**(5) 2813–2831 URL https://link.aps.org/doi/10.1103/PhysRevB.41.2813
[6] Hinuma Y, Oba F and Tanaka I 2013 *Phys. Rev. B* **88**(7) 075319 URL https://link.aps.org/doi/10.1103/PhysRevB.88.075319
[7] Lany S, Osorio-Guillén J and Zunger A 2007 *Phys. Rev. B* **75**(24) 241203 URL https://link.aps.org/doi/10.1103/PhysRevB.75.241203
[8] Hinuma Y, Oba F, Kumagai Y and Tanaka I 2013 *Phys. Rev. B* **88**(3) 035305 URL https://link.aps.org/doi/10.1103/PhysRevB.88.035305
[9] Grüneis A, Kresse G, Hinuma Y and Oba F 2014 *Phys. Rev. Lett.* **112**(9) 096401 URL http://link.aps.org/doi/10.1103/PhysRevLett.112.096401
[10] Hinuma Y, Grüneis A, Kresse G and Oba F 2014 *Phys. Rev. B* **90**(15) 155405 URL https://link.aps.org/doi/10.1103/PhysRevB.90.155405
[11] Hinuma Y, Kumagai Y, Tanaka I and Oba F 2017 *Phys. Rev. B* **95**(7) 075302 URL https://link.aps.org/doi/10.1103/PhysRevB.95.075302
[12] Lambrecht W R L and Punya A 2013 Heterovalent ternary II-IV-N$_2$ compounds: perspectives for a new class of wide-band-gap nitrides *III-Nitride Semiconductors and their Modern Devices* ed Gill B (Oxford University Press) pp 519–585
[13] Lyu S, Skachkov D, Kash K, Blanton E W and Lambrecht W R L 2019 *Physica Status Solidi (a)* **216** 1800875 URL https://doi.org/10.1002/pssa.201800875
[14] Punya A and Lambrecht W R L 2013 *Physical Review B* **88** URL https://doi.org/10.1103/physrevb.88.075302

[15] Han L, Kash K and Zhao H 2016 *J. Appl. Phys.* **120** 103102 URL https://aip.scitation.org/doi/abs/10.1063/1.4962280

[16] Han L, Lieberman C and Zhao H 2017 *Journal of Applied Physics* **121** 093101 URL https://doi.org/10.1063/1.4977696

[17] Han L, Lieberman C and Zhao H 2017 *Journal of Applied Physics* **121** 093101 URL https://doi.org/10.1063/1.4977696

[18] Hohenberg P and Kohn W 1964 *Phys. Rev.* **136** B864–B871

[19] Kohn W and Sham L J 1965 *Phys. Rev.* **140** A1133–A1138

[20] van Schilfgaarde M, Kotani T and Faleev S 2006 *Phys. Rev. Lett.* **96** 226402

[21] Kotani T, van Schilfgaarde M and Faleev S V 2007 *Phys.Rev. B* **76** 165106 (pages 24) URL http://link.aps.org/abstract/PRB/v76/e165106

[22] Schlegel H B 1982 *J. Comp. Chem.* **3** 214–218

[23] Torrent M, Jollet F, Bottin F, Zérah G and Gonze X 2008 *Computational Materials Science* **42** 337–351 URL https://doi.org/10.1016/j.commatsci.2007.07.020

[24] Garrity K F, Bennett J W, Rabe K M and Vanderbilt D 2014 *Computational Materials Science* **81** 446–452 URL https://doi.org/10.1016/j.commatsci.2013.08.053

[25] Hartwigsen C, Goedecker S and Hutter J 1998 *Physical Review B* **58** 3641–3662 URL https://doi.org/10.1103/physrevb.58.3641

[26] Methfessel M, van Schilfgaarde M and Casali R A 2000 A Full-Potential LMTO Method Based on Smooth Hankel Functions *Electronic Structure and Physical Properties of Solids. The Use of the LMTO Method* (*Lecture Notes in Physics* vol 535) ed Dreyssé H (Berlin Springer Verlag) p 114

[27] Kotani T and van Schilfgaarde M 2010 *Phys. Rev. B* **81** 125117

[28] Bhandari C, van Schilgaarde M, Kotani T and Lambrecht W R L 2018 *Physical Review Materials* **2** URL https://doi.org/10.1103/physrevmaterials.2.013807

[29] Moses P G, Miao M, Yan Q and de Walle C G V 2011 *The Journal of Chemical Physics* **134** 084703 URL https://doi.org/10.1063/1.3548872

[30] Lyu S and Lambrecht W R L 2017 *Phys. Rev. Materials* **1**(2) 024606 URL https://link.aps.org/doi/10.1103/PhysRevMaterials.1.024606

[31] Jaroenjittichai A P and Lambrecht W R L 2016 *Phys. Rev. B* **94**(12) 125201 URL http://link.aps.org/doi/10.1103/PhysRevB.94.125201

[32] Lyu S and Lambrecht W R 2019 *Solid State Communications* **299** 113664 ISSN 0038-1098 URL http://www.sciencedirect.com/science/article/pii/S0038109819302911

[33] Kuo C T, Chang K K, Shiu H W, Liu C R, Chang L Y, Chen C H and Gwo S 2011 *Applied Physics Letters* **99** 122101 URL https://doi.org/10.1063/1.3641422

[34] Jaroenjittichai A P, Lyu S and Lambrecht W R L 2017 *Phys. Rev. B* **96**(7) 079907(E) URL https://link.aps.org/doi/10.1103/PhysRevB.96.079907

[35] Jaroenjittichai A P, Lyu S and Lambrecht W R L 2017 *Phys. Rev. B* **96**(7) 079907 URL https://link.aps.org/doi/10.1103/PhysRevB.96.079907

[36] Liu J W, Kobayashi A, Toyoda S, Kamada H, Kikuchi A, Ohta J, Fujioka H, Kumigashira H and Oshima M 2011 *Physica Status Solidi (b)* **248** 956–959 URL https://onlinelibrary.wiley.com/doi/abs/10.1002/pssb.201046459

[37] Wang T, Ni C and Janotti A 2017 *Phys. Rev. B* **95**(20) 205205 URL https://link.aps.org/doi/10.1103/PhysRevB.95.205205

[38] Veal T D, King P D C, Hatfield S A, Bailey L R, McConville C F, Martel B, Moreno J C, Frayssinet E, Semond F and Zúñiga Pérez J 2008 *Applied Physics Letters* **93** 202108 URL https://doi.org/10.1063/1.3032911

[39] Friedrich C, Müller M C and Blügel S 2011 *Phys. Rev. B* **83**(8) 081101 URL https://link.aps.org/doi/10.1103/PhysRevB.83.081101

[40] Arca E, Fioretti A, Lany S, Tamboli A C, Teeter G, Melamed C, Pan J, Wood K N, Toberer E and Zakutayev A 2018 *IEEE Journal of Photovoltaics* **8** 110–117 ISSN 2156-3381